Article

# Earliest evidence of making fire

https://doi.org/10.1038/s41586-025-09855-6

Received: 5 November 2024

Accepted: 4 November 2025

Published online: 10 December 2025

Check for updates

Rob Davis[1], Marcus Hatch[2], Sally Hoare[3], Simon G. Lewis[2], Claire Lucas[1], Simon A. Parfitt[4,5], Silvia M. Bello[5], Mark Lewis[5], Jordan Mansfield[6], Jens Najorka[7], Simon O'Connor[1], Sylvia Peglar[8,10], Andrew Sorensen[9], Chris Stringer[5] & Nick Ashton[1,4]✉

Fire-making is a uniquely human innovation that stands apart from other complex behaviours such as tool production, symbolic culture and social communication. Controlled fire use provided adaptive opportunities that had profound effects on human evolution. Benefits included warmth, protection from predators, cooking and creation of illuminated spaces that became focal points for social interaction[1–3]. Fire use developed over a million years, progressing from harvesting natural fire to maintaining and ultimately making fire[4]. However, determining when and how fire use evolved is challenging because natural and anthropogenic burning are hard to distinguish[5–7]. Although geochemical methods have improved interpretations of heated deposits, unequivocal evidence of deliberate fire-making has remained elusive. Here we present evidence of fire-making on a 400,000-year-old buried landsurface at Barnham (UK), where heated sediments and fire-cracked flint handaxes were found alongside two fragments of iron pyrite—a mineral used in later periods to strike sparks with flint. Geological studies show that pyrite is locally rare, suggesting it was brought deliberately to the site for fire-making. The emergence of this technological capability provided important social and adaptive benefits, including the ability to cook food on demand—particularly meat—thereby enhancing digestibility and energy availability, which may have been crucial for hominin brain evolution[3].

Determining when humans first controlled fire is a critical area of research for understanding human biological, technological and social evolution[1–3]. Rather than originating with the ability to produce fire, human fire use probably began with the opportunistic exploitation of natural wildfires, eventually progressing to deliberate harvesting and maintenance of fire[4]. Archaeological evidence for early fire use is limited and often ambiguous, typically consisting of associations between heated materials and stone tools. Notable examples include open-air sites in Kenya, such as Chesowanja[8] and Koobi Fora[9,10] dating to 1.6–1.4 million years ago (Ma), cave deposits in South Africa at Swartkrans[11] and Wonderwerk[12] around 1.0–0.8 Ma, and lake-edge settings at Gesher Benot Ya'aqov[13] in Israel dated to approximately 0.78 Ma. However, these instances are difficult to interpret[5–7].

Early humans who relied on naturally occurring fire faced substantial challenges. Wildfires, sparked primarily by lightning strikes, are often seasonal and unpredictable, particularly in mid-latitudes[4]. Sustained fire use would have required improved social coordination, including a more complex division of labour, with people shifting effort from traditional activities such as hunting and foraging to the transportation and maintenance of fire[14]. The ability to create fire when and where it was needed would have reduced these costs significantly and enabled more efficient fuel use, particularly in environments where combustible material was scarce[15]. Thus, identifying when humans developed fire-making abilities marks a pivotal moment in human development.

In Europe there are occasional signals of fire use from around 400 thousand years ago (ka) (Fig. 1a). These include the cave sites of Menez-Dregan (France)[16] and Gruta da Aroeira (Portugal)[17], and open-air locations of Terra Amata (France)[18], La Cansaladeta (Spain)[19], Medzhibozh (Ukraine)[20] and Beeches Pit (UK)[21]. By 350–200 ka, there appears to be more widespread use of fire in Europe, the Levant and Africa[2]. Although this distribution suggests increasingly regular fire use, direct evidence of fire-making by pre-*Homo sapiens* hominins has, until recently, been limited to a few dozen handaxes from several French Neanderthal sites, dating to around 50 ka, that exhibit use-wear traces consistent with experimental tools that were struck with pyrite to create sparks[22]. Barnham—the site presented here—suggests that fire-making is considerably earlier, at more than 400 ka.

## The Barnham site context

The Palaeolithic site of East Farm Barnham (52° 22′ 29″ N, 0° 45′ 14″ E) lies within a disused clay pit in the Breckland of Suffolk, UK (Fig. 1 and Extended Data Fig. 1a). Following previous work in the early twentieth century, more extensive excavations were undertaken in 1989–1994 (ref. 23) and currently since 2013 (ref. 24). The Pleistocene deposits occupy a small basin, formed within a glacial channel cut into Chalk bedrock. From the base, the glacial deposits (units 1–3) are overlain by interglacial sediments, which, at the southern edge of the basin, are decalcified and comprised of a coarse lag gravel (unit 4), less than

[1]Department Britain, Europe and Prehistory, British Museum, London, UK. [2]School of Geography, Queen Mary University of London, London, UK. [3]Department of Archaeology, Classics and Egyptology, HLC, University of Liverpool, Liverpool, UK. [4]Institute of Archaeology, University College London, London, UK. [5]CHER, Natural History Museum, London, UK. [6]Independent researcher, Campagnac-lès-Quercy, France. [7]Core Research Laboratories, Natural History Museum, London, UK. [8]Independent researcher, Cambridge, UK. [9]Faculty of Archaeology, University of Leiden, Leiden, The Netherlands. [10]Deceased: Sylvia Peglar. ✉e-mail: nashton@britishmuseum.org

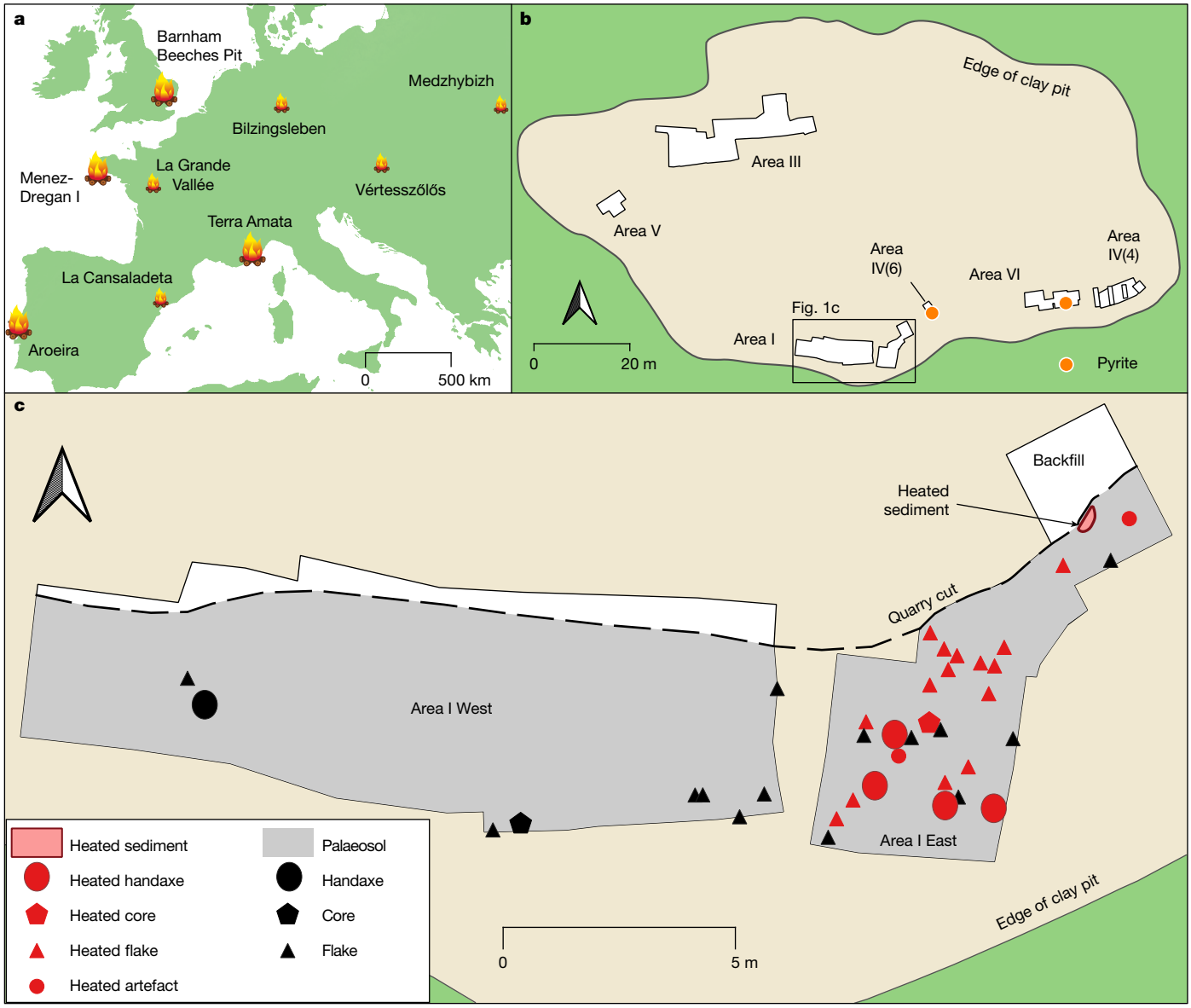


**Fig. 1 | Location and site plans of Barnham. a**, Key sites in Europe with evidence of fire use, probably dating to MIS 11. Large fire symbols indicate strong evidence; small fire symbols indicate more equivocal evidence of fire use, and/or greater chronological uncertainty. **b**, Plan of Barnham clay pit highlighting the main excavated areas. **c**, Plan of Area I showing the distribution of artefacts within the palaeosol (unit 6). Base map from Natural Earth (https://www.naturalearthdata.com/).

30 cm of fluvial sand (unit 5e) and less than 10 cm of black clay identified as a palaeosol (unit 6) (Extended Data Fig. 1b). The middle of the basin has stratigraphically equivalent, but laterally variable deposits. Here the lag gravel thins out from the southern edge, whereas the silty sand thickens to a more complex 5-m deep sequence of predominantly silts and clays (unit 5c) that are calcareous with organic remains. The palaeosol (unit 6) survives in places overlying unit 5c (Extended Data Fig. 1b). Pollen, molluscs and vertebrates from unit 5c indicate it was a stream-fed pond, surrounded by grass and deciduous woodland, which infilled during the first half of an interglacial. After the pond dried out and the palaeosol formed, more than 3 m of predominantly colluvial brown silty clay (unit 7) infilled the basin. The age of the site is based on lithostratigraphy, geochronology and biostratigraphy[23–26] (Extended Data Fig. 1b). The glacial deposits are attributed to the Anglian glaciation, marine isotope stage (MIS) 12, around 478–427 ka and the overlying lacustrine sediments to the first half of the Hoxnian interglacial (MIS 11c; around 427–415 ka) (Supplementary Information, section 3).

Two archaeological assemblages have been recovered from the site. The first consists of cores, flakes and flake tools from units 4, 5c and 5e, whereas the second from the palaeosol (unit 6) includes handaxes and flakes from their manufacture. This suggests a succession of two culturally distinct human groups occupying the site, the first during the early temperate phase (pollen zone HoII) and the second probably during the peak interglacial (pollen zone HoII/III) of the Hoxnian[24].

Heated materials are associated predominantly with the second assemblage, either on or within the palaeosol along the southern fringe of the basin. These include natural flint, artefactual flint and sediment. The rarity of charcoal and absence of ash may be attributed to erosion caused by wind and rain, whereas the lack of burnt bone is due to decalcification in this part of the site. Marked concentrations of heated flint occur at the eastern end of the site (Area VI), but there is no clear indication of heated sediment. The only area where heated sediment has been identified definitively is in Area I East. Here, a concentrated zone of reddened clayey silt (RCS) was found within the palaeosol, with fragments of reddened sediment dispersed in the

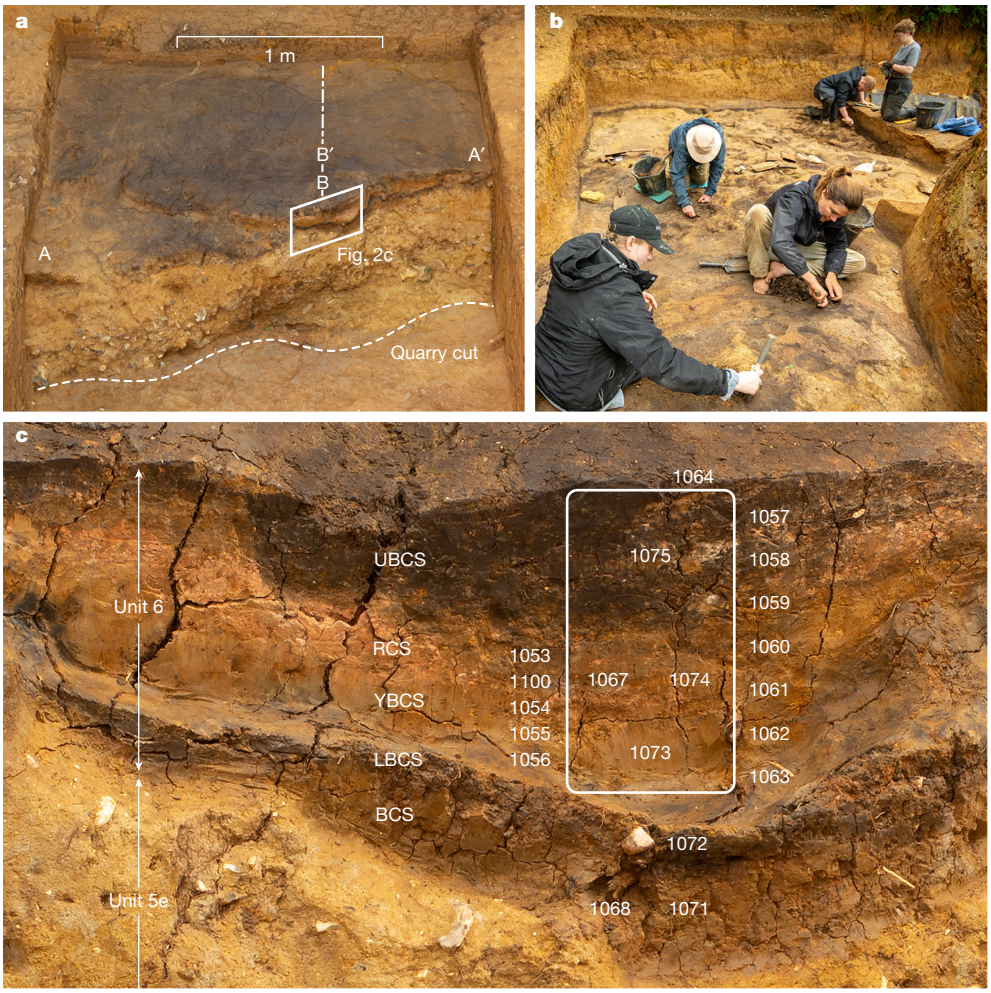


**Fig. 2 | Photographs of excavation of Area 1 East. a**, Before excavation in 2022 from north–west, showing truncation by commercial excavation of RCS within palaeosol complex. Sections A–A′, B–B′ and position of sampling column are indicated. **b**, Adjacent area from north under excavation in 2024. **c**, Partly excavated RCS within palaeosol complex in 2023 from north-west showing sampling locations and column.

surrounding matrix. These sediments were truncated on the northern side when the pit was commercially active, creating a section (A–A′: Fig. 2a). The sediments in A–A′ show the top of the lag gravel (unit 4), roughly 20 cm of yellow silty sand (unit 5e) and the overlying palaeosol (unit 6). Here the palaeosol is a complex unit of five main subdivisions, comprising, from the base: brown clayey silt (BCS); lower black clayey silt (LBCS); yellowish-brown clayey silt (YBCS); RCS and upper black clayey silt (UBCS) (Fig. 2a,c). The YBCS is interpreted as the unheated equivalent of the RCS. In section, the RCS was 55 cm across and up to 8 cm thick. Its lateral extent was difficult to define clearly, due partly to patches and fragments of RCS above and around the main concentration. The area was excavated using diagonally opposed quadrants (Supplementary Fig. 1.1), which revealed that the main concentration of reddening was in the north–south section (B–B′) and that its extent was around 55 × 30 cm, with considerable truncation at the northern edge.

Previous excavation of Area I West established that artefacts were rare within the palaeosol. However, in the area adjacent to the RCS in Area I East, artefact density is much higher (Fig. 1c). Notably, 76% of artefacts in Area I East show clear evidence of heating, such as cracking/crazing, reddening and spalling, including one core, 19 flakes and four handaxes (Fig. 4a and Extended Data Fig. 2). By contrast, in Area I West only one unheated handaxe was recovered from previous excavations of the palaeosol horizon. The concentration of heat-shattered handaxes and other artefacts near the RCS marks the area as functionally distinct from other parts of the site.

## Analyses of reddened sediment

Four separate studies were conducted to analyse the RCS from section A–A′ (Fig. 2c), aiming to determine whether the sediments had been subjected to heating and, if so, whether it was likely to have been caused by natural fire or human activity.

### Micromorphology

Micromorphological analysis was undertaken on two thin sections from the RCS (Supplementary Information, section 4). The reddening is attributable to the formation of haematite—a mineral produced through heating of iron-rich sediments. Its distribution is homogeneous and not associated with particular microfacies or voids, indicating that it was preserved in situ. However, the reddening is interrupted locally by clay illuviation in channels and voids. This clay illuviation is linked to pedogenic processes in the overlying UBCS and exhibits an orange hue associated with natural iron oxidation. The mixing of the heat-related reddening with post-depositional clay illuviation may account for some of the magnetic properties and the mixed heating signal observed in the Fourier-transform infrared spectroscopy (FTIR) analysis described below. Two further micromorphology samples from unit 6, one adjacent to the concentrated area of RCS (at B′; Fig. 2a and Supplementary Fig. 1.1), showed no indications of heating, supporting the interpretation that the heated sediment represents a localized and isolated patch (Fig. 3).

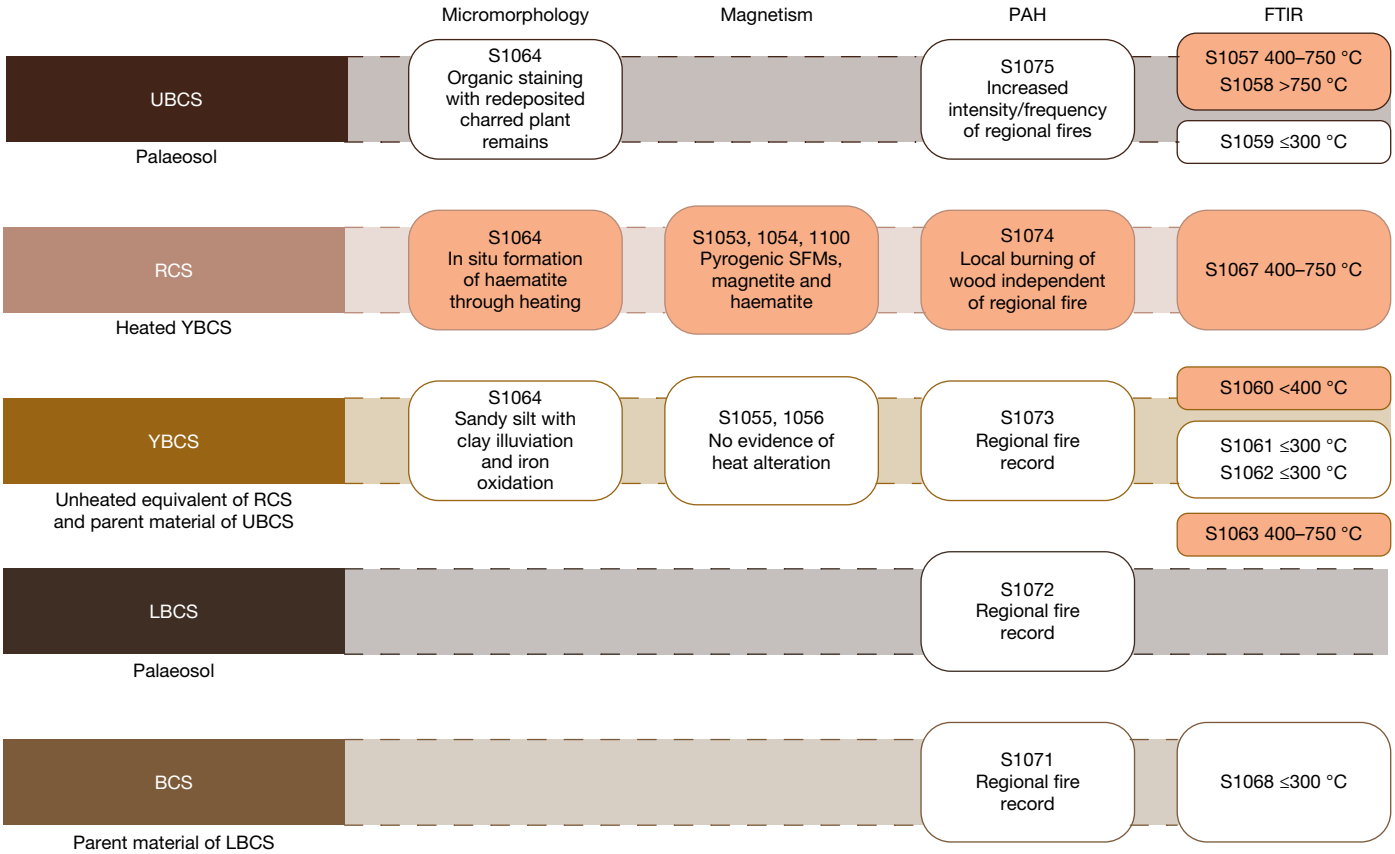


**Fig. 3 | Schematic diagram through palaeosol complex with analytical results.** Results are for micromorphology, magnetic properties, PAH and FTIR spectroscopy. Sample locations shown in Fig. 2c.

### Environmental magnetism

Three samples were taken from the RCS and two from the adjacent YBCS, which served as unheated control samples. The magnetic properties of the RCS (Supplementary Information, section 5) differ markedly from those of the unheated control samples, exhibiting elevated levels of secondary fine-grained ferrimagnetic and superparamagnetic minerals of pyrogenic origin, unlike the control samples. To assess whether these characteristics could result from heating, a series of experiments of single and multiple heating events of varying durations, was conducted. The aim was to determine whether the reddening could have arisen from one or multiple heating events, as repeated, localized burning is more typical of human than natural fire events (S.H. et al. manuscript in preparation).

The closest experimental analogue in terms of the minerology and grain size distribution, was observed after 12 or more heating events, each lasting 4 h at temperatures of 400 °C or 600 °C. Although the archaeological samples exhibit substantially lower magnetic susceptibility values, this may result from post-depositional mixing with unheated illuviated clay. Overall, the experiments indicate that the magnetic properties of the RCS result from an indeterminate number of short-duration heating events, consistent with repeated human use (Fig. 3).

### Polycyclic aromatic hydrocarbons

Nine samples from units 5e, 6 and 7 were analysed to establish the polycyclic aromatic hydrocarbons (PAH) record of Area I sediments (Supplementary Information, section 6). Of these, only the RCS (sample 1074) exhibits a higher abundance of heavy (h)PAHs relative to light (l)PAHs. The hPAH distribution in this sample closely resembles that associated with human fire use, as documented in both experimental and archaeological hearths, compared with natural fires associated with a predominance of lPAHs[27,28].

Statistical analysis of individual PAH compounds can be used to examine links between localized fires (human or natural) and regional wildfires[27]. In the YBCS (sample 1073), there is a strong correlation between lPAHs and hPAHs, suggesting that local fire signals in this unit were linked to the regional wildfire regime. In contrast, no statistical correlation exists among the PAH compounds in the RCS, despite it being part of the same sedimentary unit. This lack of correlation indicates a distinct PAH source, most probably resulting from local wood burning unrelated to the frequency and/or intensity of natural fires on the regional scale (Fig. 3).

### Fourier-transform infrared spectroscopy

Nine samples from the five subunits of unit 6 were analysed using FTIR spectroscopy, preferentially selecting visually reddened components that varied in abundance across the subunits (Supplementary Information, section 7). Experimental heating of a reference sample from the YBCS was conducted to establish baseline FTIR responses to heating at known temperatures. These spectra showed changes in common clay absorption bands when heated between 150 and 1,000 °C. When compared against this experimental reference, five samples from Area I (1063, 1060, 1067, 1058 and 1057) exhibited clear evidence of heating, corresponding to temperature ranges of less than 400 °C, 400–750 °C and more than 750 °C (Fig. 3). The remaining four samples (1068, 1062, 1061 and 1059) showed no signs of thermal alteration. Although some admixture of heated and unheated sediment seems to be present in four of the five heated samples, they all displayed consistent alterations in the three diagnostic clay absorption bands, aligning with heating respective to increasing temperatures.

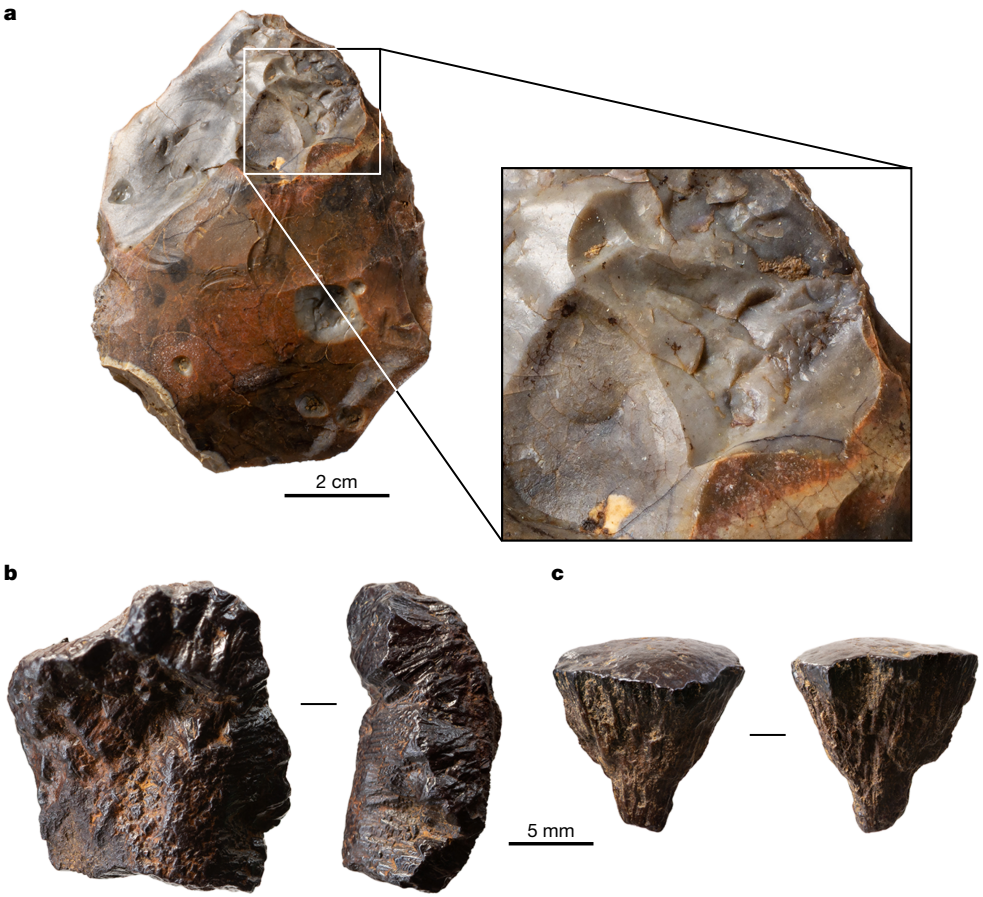


**Fig. 4 | Handaxe and pyrite fragments from palaeosol. a**, Heat-altered handaxe from palaeosol in Area I East with close-up of fractured surface caused by fire. **b**, Fragment of pyrite found on the surface of palaeosol in Area IV(6). **c**, Fragment of pyrite from palaeosol in Area VI, found in association with concentrations of heated flint.


## Summary

A discrete patch of reddened sediment, associated with a concentration of lithic artefacts, including four heat-shattered handaxes, was formed in situ through localized burning of wood. Micromorphological analysis indicates preservation of the heating signature within the palaeosol; FTIR results demonstrate that temperatures exceeded 750 °C in some samples; and magnetic and PAH analyses suggest that the fire activity was recurrent, spatially confined and decoupled from the regional wildfire regime. Together, these analyses provide clear evidence of in situ heating of sediment that is likely to be related to anthropogenic activity, representing the maintenance of a combustion feature.


## Pyrite

An additional line of evidence potentially indicative of human fire use at Barnham is the presence of two small fragments of oxidized pyrite ($FeS_2$) derived from shattered nodules (Fig. 4b,c). Both fragments retain a portion of their original cortical surface, while their interior fracture faces exhibit characteristic pseudomorphs after radially grown pyrite. Micro X-ray diffraction (XRD) analyses identified goethite (FeOOH) as the dominant phase, with minor haematite ($Fe_2O_3$) detected in some spots, confirming complete oxidation of the pyrite.

The first fragment (Fig. 4c and Supplementary Fig. 2.1) was found within the palaeosol in Area VI, in close association with concentrations of heated natural flint and lithic artefacts. Its broken surfaces show a well-developed radial structure composed of elongated crystals radiating outward from a central point. The homogenous structure indicates that the pseudomorphic pyrite to goethite replacement occurred under relatively stable conditions.

The second fragment (Fig. 4b and Supplementary Fig. 2.2) was found on the surface of the palaeosol in Area IV(6). Although it may not be in primary context, it is likely to have derived from the palaeosol. This specimen has a more heterogeneous internal structure, consisting of intersecting domains of subparallel prismatic crystals, with polygonal terminations. A partial radial pattern is preserved within one domain. In contrast to the first fragment, the innermost region of this piece displays higher porosity and relict features of the original pyrite crystals, indicating longer exposure above ground.

The occurrence of pyrite at Barnham warrants further consideration. Pyrite is a naturally occurring iron sulfide mineral that can be struck against flint to produce sparks to ignite tinder. Its use for this purpose is well documented in ethnographic accounts worldwide[29]. Pyrite has been recovered from European archaeological sites dating from the late Middle Palaeolithic to the historic periods, occasionally bearing wear traces consistent with use for fire-making and, in some cases, found in association with flint striking tools[22,30,31].

Geologically, pyrite occurs within a broad range of deposits, including Cretaceous Chalk, where it forms diagenetically as crystalline nodules. Its formation within the Chalk is stratigraphically and regionally variable across the UK, where it is found predominantly in the Lower Chalk due to more favourable anoxic conditions, as compared with the Middle and Upper Chalk[32]. Although pyrite readily oxidizes and degrades upon exposure to air and moisture, it remains relatively common in exposed coastal cliffs, particularly in Kent and Yorkshire[32]. Despite the Breckland being underlain by Chalk bedrock, pyrite is rare locally. The only documented occurrence of pyrite in the Geological

Memoirs of the area is from a Chalk quarry at Stowlangtoft, 12 km south-east of Barnham, where pyrite is noted within the Lower Chalk and, in an oxidized form, within the Upper Chalk[33].

The rarity of pyrite around Barnham may be related to the considerable depth of the Lower Chalk, which dips at around 1° eastwards from a surface exposure 15 km to the west, placing it at around 70 m depth beneath Barnham[34] (Extended Data Fig. 1a). As a result, the Lower Chalk in the Breckland was not incised by pre-Anglian or post-Anglian rivers, although it was probably influenced by Anglian glacial processes. The resulting till and glacio-fluvial gravels could serve as potential secondary sources for pyrite. However, for pyrite to have been accessible to early humans, these glacial deposits would have needed to undergo surface erosion or be reworked into tertiary contexts, such as Hoxnian river sediments.

The rarity of pyrite in the Breckland region is supported by extensive lithological studies of the regional Pleistocene geology. Analysis of over 121,000 individual clasts from 26 sites, including pre-Anglian fluvial gravels, Anglian glacial sediments and post-Anglian fluvial gravels, provides a robust dataset, with more than 33,000 clasts specifically from the Barnham area (Supplementary Information, section 3). None of the samples contained pyrite fragments, demonstrating the extreme rarity of this mineral in Pleistocene deposits in the region. Based on this evidence, we interpret that the pyrite found at Barnham was transported to the site from outside the Breckland. Furthermore, its presence within a predominantly stone-free palaeosol, closely associated with heated artefacts and a hearth, strongly suggests intentional introduction for fire-making.

## Discussion

The heated sediment in Area I provides the most compelling evidence for anthropogenic fire maintenance at Barnham. Concentrations of heated flint in Area VI, located 45 m to the east, hint at the presence of additional hearths that have not been preserved, further supporting the evidence of persistent fire use at the site. Of importance is other evidence of fire use in the Breckland during MIS 11 (Extended Data Fig. 1a). At Beeches Pit, 10 km south-west of Barnham, at least three distinct burning horizons, including probable hearths and heated artefacts, have been identified and correlated with the upper part of units 5 and 6 at Barnham through molluscan biostratigraphy[21,35]. Similarly, at Devereux's Pit just 500 m west of Beeches Pit, and also dating to MIS 11, ongoing excavations have revealed heated flint artefacts (R.D. et al., manucript in preparation). Notably, all three sites occupy marginal locations, away from the main river valleys and associated with small ponds or springs. In the absence of caves, these locations probably provided safer, more sheltered environments for domestic activities. Taken together, these findings present a strong case for controlled fire use across the Breckland region during MIS 11.

The advantage of fire-making lies in its predictability, which facilitated better planning of seasonal routines, the establishment of domestic sites in preferred locations and increased structuring of the landscape through enculturation. Year-round access to fire would have provided an enhanced communal focus, potentially as a catalyst for social evolution[36]. It would have enabled routine cooking, could have expanded the consumption of roots, tubers and meat, reduced energy required for digestion and increased protein intake[3]. These dietary improvements may have contributed to increase in brain size[37], enhanced cognition and the development of more complex social relationships, as articulated in the Social Brain Hypothesis[38]. Moreover, controlled fire use was instrumental in advancing other technologies, such as the production of glues for hafting. The widespread appearance of Levallois points from Africa to Eurasia by MIS 7 (243–191 ka), often interpreted as spear-tips[39–41], provides strong evidence of effective hafting. This interpretation is supported by use-wear evidence[42] and the identification of heat-synthesized birch bark tar as a stone tool adhesive[43].

The evidence from Barnham strongly indicates complex behaviour, including an understanding of the properties of pyrite, knowledge of suitable tinder for successful ignition and the curation of pyrite as part of a fire-making kit. This evidence sits alongside other markers of sophisticated human behaviour during the late Middle Pleistocene, including bone[44] and wood-working[45], as well as the manufacture of adhesives for hafting[43]. Collectively, these developments suggest a major transition in human behaviour from around 500 ka to 300 ka—a period marked by a steady increase in brain size approaching modern levels[37]. Although these behavioural and cognitive changes certainly involved early Neanderthals and other lineages of contemporaneous humans in western Eurasia, it is likely that similar developments occurred among the ancestors of Denisovans in eastern Eurasia and of *Homo sapiens* in Africa.

## Online content

Any methods, additional references, Nature Portfolio reporting summaries, source data, extended data, supplementary information, acknowledgements, peer review information; details of author contributions and competing interests; and statements of data and code availability are available at https://doi.org/10.1038/s41586-025-09855-6.


1. Perles, C. *La Prehistoire du Feu* (Masson, 1977).
2. Roebroeks, W. & Villa, P. On the earliest evidence for habitual use of fire in Europe. *Proc. Natl Acad. Sci. USA* **108**, 5209–5214 (2011).
3. Wrangham, R. Control of fire in the Paleolithic: evaluating the cooking hypothesis. *Curr. Anthrop.* **58**, S303–S313 (2017).
4. Gowlett J. A. J. in *Sur le chemin de l'humanité. Via humanitatis: les grandes étapes de l'évolution morphologique et culturelle de l'Homme: émergence de l'être humain* (ed. de Lumley, H.) 171–197 (Académie Pontificale des Sciences/CNRS, 2015).
5. James, S. R. Hominid use of fire in the Lower and Middle Pleistocene: s review of the evidence. *Curr. Anthropol.* **30**, 1–26 (1989).
6. Sandgathe, D. M. et al. Timing of the appearance of habitual fire use. *Proc. Natl Acad. Sci. USA* **108**, E298 (2011).
7. Goldberg, P., Miller, C. E. & Mentzer, S. M. Recognizing fire in the Paleolithic archaeological record. *Curr. Anthrop.* **58**, S175–S190 (2017).
8. Gowlett, J. A. J. et al. Early archaeological sites, hominid remains and traces of fire from Chesowanja, Kenya. *Nature* **294**, 125–129 (1981).
9. Bellomo, R. V. Methods of determining early hominid behavioural activities associated with the controlled use of fire at FxJj 20 Main, Koobi Fora, Kenya. *J. Hum. Evol.* **27**, 173–195 (1994).
10. Hlubik, S. et al. Researching the Nature of fire at 1.5 Mya on the site of FxJj20 AB, Koobi Fora, Kenya, using high-resolution spatial analysis and FTIR spectrometry. *Curr. Anthrop.* **58**, S243–S257 (2017).
11. Brain, C. K. & Sillen, A. Evidence from the Swartkrans cave for the earliest use of fire. *Nature* **336**, 464–466 (1988).
12. Berna, F. et al. Microstratigraphic evidence of in situ fire in the Acheulean strata of Wonderwerk Cave, Northern Cape province, South Africa. *Proc. Natl Acad. Sci. USA* **109**, E1215–E1220 (2012).
13. Alperson-Afil, N., Richter, D. & Goren-Inbar, N. Phantom hearths and the use of fire at Gesher Benot Ya'aqov, Israel. *PaleoAnthrop.* **2007**, 1–15 (2007).
14. Chazan, M. Toward a long prehistory of Fire. *Curr. Anthrop.* **58**, S351–S359 (2017).
15. Sorensen, A. C. On the relationship between climate and Neandertal fire use during the Last Glacial in south-west France. *Quat. Int.* **436A**, 114–128 (2017).
16. Ravon, A.-L. in *Crossing the Human Threshold. Dynamic Transformation and Persistent Places during the Middle Pleistocene* (eds Pope, M. et al.) 106–122 (Routledge, 2018).
17. Sanz, M. et al. Early evidence of fire in south-western Europe: the Acheulean site of Gruta da Aroeira (Torres Novas, Portugal). *Sci. Rep.* **10**, 12053 (2020).
18. de Lumley, H. *Terra Amata, Nice, Alpes-Maritimes, France, Tome V: Comportement et Mode de Vie des Chasseurs Acheuléens de Terra Amata* (Editions CNRS, 2016).
19. Ollé, A. et al. The Middle Pleistocene site of La Cansaladeta (Tarragona, Spain): stratigraphic and archaeological succession. *Quat. Int.* **393**, 137–157 (2016).
20. Stepanchuk, V. N. & Moigne, A.-M. MIS 11-locality of Medzhibozh, Ukraine: Archaeological and paleozoological evidence. *Quat. Int.* **409**, 241–254 (2016).
21. Gowlett, J. A. J. et al. Beeches Pit – archaeology, assemblage dynamics and early fire history of a Middle Pleistocene site in East Anglia, UK. *Eurasian Prehist.* **3**, 3–38 (2005).
22. Sorensen, A. C., Claude, E. & Soressi, M. Neandertal fire-making technology inferred from microwear analysis. *Sci. Rep.* **8**, 10065 (2018).
23. Ashton, N. M., Lewis, S. G. & Parfitt, S. A. *Excavations at Barnham, Suffolk, 1989-94* (British Museum, 1998).
24. Ashton, N. M. et al. Handaxe and non-handaxe assemblages during Marine Isotope Stage 11 in northern Europe: Recent investigations at Barnham, Suffolk, UK. *J. Quat. Sci.* **31**, 837–843 (2016).
25. Preece, R. C. & Penkman, K. E. H. New faunal analyses and amino acid dating of the Lower Palaeolithic site at East Farm, Barnham, Suffolk. *Proc. Geol. Assoc.* **116**, 363–377 (2005).
26. Voinchet, P. et al. New chronological data (ESR and ESR/U-series) for the earliest Acheulean sites of northwestern Europe. *J. Quat. Sci.* **30**, 610–622 (2015).

27. Brittingham, A. et al. Geochemical evidence for the control of fire by Middle Palaeolithic hominins. *Sci. Rep.* **9**, 15368 (2019).
28. Denis, E. H. et al. Polycyclic aromatic hydrocarbons (PAHs) in lake sediments record historic fire events: validation using HPLC-fluorescence detection. *Org. Geochem.* **45**, 7–17 (2012).
29. Hough, W. *Fire-making Apparatus in the United States National Museum* (United States Government Printing Office, 1928); https://archive.org/details/firemakingappara0000walt.
30. Stapert, D. & Johansen, L. Flint and pyrite: making fire in the Stone Age. *Antiq.* **73**, 765–777 (1999).
31. Sorensen, A. C., Roebroeks, W. & Van Gijn, A.-L. Fire production in the deep past: the expedient strike-a-light model. *J. Archaeol. Sci.* **42**, 476–486 (2014).
32. Jeans, C. V., Turchyn, A. V. & Hu, X.-F. Sulfur isotope patterns of iron sulfide and barite nodules in the Upper Cretaceous Chalk of England and their regional significance in the origin of coloured chalks. *Acta Geologica Polonica* **66**, 227–256 (2016).
33. Bristow, C. R. 1990. *Geology of the Country around Bury St Edmunds*. Memoir British Geological Survey, Sheet 189 (England and Wales) (British Geological Survey, 1990).
34. Ander, E. L. et al. *Baseline Report Series 13: The Great Ouse Chalk aquifer, East Anglia*. Commissioned Report CR/04/236N (British Geological Survey, 2004).
35. Preece, R. C. et al. Terrestrial environments during MIS 11: evidence from the Palaeolithic site at West Stow, Suffolk, UK. *Quat. Sci. Rev.* **26**, 1236–1300 (2007).
36. Wiessner, P. W. Embers of society: Firelight talk among the Ju/'hoansi Bushmen. *Proc. Natl Acad. Sci. USA* **111**, 14027–14035 (2014).
37. Gingerich, P. D. Pattern and rate in the Plio-Pleistocene evolution of modern human brain size. *Sci. Rep.* **12**, 11216 (2022).
38. Dunbar, R. I. M. The social brain hypothesis. *Evol. Anthrop.* **6**, 178–190 (1998).
39. Villa, P. & Lenoir, M. in *The Evolution of Hominin Diets* (eds Hublin, J-J. & Richards, M. P.) 59–85 (Springer, 2009).
40. Locht, J.-L. et al. Une occupation de la phase ancienne du Paléolithique moyen à Therdonne (Oise): chronostratigraphie, production de pointes Levallois et réduction des nucleus. *Gallia Préhistoire* **52**, 1–32 (2010).
41. Malinsky-Buller, A. The muddle in the Middle Pleistocene: the Lower–Middle Paleolithic transition from the Levantine perspective. *J. World Prehist.* **29**, 1–78 (2016).
42. Rots, V. Insights into early Middle Palaeolithic tool use and hafting in Western Europe. The functional analysis of level {IIa} of the early Middle Palaeolithic site of Biache-Saint-Vaast (France). *J. Archaeol. Sci.* **40**, 497–506 (2013).
43. Mazza, P. et al. A new Palaeolithic discovery: tar-hafted stone tools in a European Mid-Pleistocene bone-bearing bed. *J. Archaeol. Sci.* **33**, 1310–1318 (2006).
44. Parfitt, S. A. & Bello, S. M. Bone tools, carnivore chewing and heavy percussion: assessing conflicting interpretations of Lower and Upper Palaeolithic bone assemblages. *R. Soc. Open Sci.* **11**, 231163 (2024).
45. Milks, A. et al. A double-pointed wooden throwing stick from Schöningen, Germany: results and new insights from a multianalytical study. *PLoS ONE* **18**, e0287719 (2023).

# Methods

### Micromorphology

Micromorphological analysis is used to investigate sediment structure and, in this case, evidence for potential hearth features. Typically, a hearth is composed of a sequence of reddened oxidized sediment overlain by a black char layer and greyish ash layer[46]. Char and ash are, however, highly susceptible to weathering and off-site transport[7], whereas cemented, reddened layers formed below fire events are more durable and have been suggested to present early evidence for fire control[8,47,48]. However, reddened sediment can also result from redoximorphic processes; thus, microcontextual analysis is needed to reveal formation and integrity[49].

To investigate the formation of the reddened sediments and of other potential microscopic combustion-related materials, seven block samples were collected for micromorphological analysis. These included two (S1064 and S1096) from the potentially heated sediment, and five (S1091, S1097, S1099, S1106 and S1107) from adjacent areas to enable comparison with non-heated sediments from the same units. For the block sample collected in 2022 (S1064), two thin sections (68 × 139 mm) were produced by the Terrascope Thin Section Slides laboratory, Troyes, France. For the remaining six samples, all collected in 2023, six thin sections (76 × 110 mm) were produced by MKFactory, Stahnsdorf, Germany, of which three (S1096, S1097 and S1106) were analysed here. Analysis was conducted with an Evident BX53 microscope and the cellSens software in plane-polarized light, cross-polarized light and oblique incident light following established descriptions[50,51].

### Environmental magnetism

Environmental magnetism uses mineral magnetic parameters as proxies to examine the neoformation, alteration and transportation of magnetic minerals in a variety of sedimentary archives, including study of Palaeolithic combustion features, where the formation and response of mineral magnetic assemblages varies under different heating conditions[17,49,52,53]. Magnetic enhancement in the surface sediments of anthropogenic and natural combustion features leads to the pyrogenic formation of fine to ultrafine secondary ferrimagnetic minerals (SFMs)[54,55]. SFMs are magnetically strong, which can cause an increase in magnetic susceptibility and frequency-dependency of magnetic susceptibility ($\chi_{FD}$)[56]. Although SFMs are formed by a variety of environmental processes (for example, heating, pedogenesis, magnetotactic bacteria and volcanic activity), it is possible to distinguish between heating and pedogenesis in soils and sediments using standard approaches[54,57]. Reductions in magnetic susceptibility values can also occur during heating due to the inversion of magnetite/maghemite to the magnetically weaker mineral haematite at higher temperatures or under conditions of heating longevity[58]. Therefore, magnetic susceptibility values can increase or decrease in response to heating.

All rocks and sediments contain varied quantities and types of magnetic minerals, the most common being iron oxides. Characterizing the response of sediment samples to laboratory-applied magnetic fields allows estimation of the composition, concentration and magnetic domain or grain size distribution of magnetic minerals, especially the iron oxides of magnetite ($Fe_3O_4$), maghemite ($\gamma Fe_2O_3$) and haematite ($\alpha Fe_2O_3$)[59]. This can be used to reconstruct past heating conditions as these oxides are linked closely to temperature, source, frequency and longevity of heating[52,54,60–63].

Sediment samples were pre-packed into 10 cc diamagnetic (plastic) pots and then subjected to the following sequence of standard magnetic measurements[64]. To assess bulk magnetic mineral concentrations, low frequency magnetic susceptibility ($\chi_{LF}$) was measured at 0.47 kHz and high frequency magnetic susceptibility ($\chi_{HF}$) at 4.7 kHz, using a Bartington MS2 meter. The difference between the two measurements gives the frequency-dependent susceptibility expressed as either mass specific property ($\chi_{FD}$) or as a percentage of $\chi_{LF}$, $\chi_{FD}$%. The loss of susceptibility between $\chi_{LF}$ and $\chi_{HF}$ reflects the response of grains that lie at the border between single domain and superparamagnetic grains[65]. Values of $\chi_{FD}$ provide an indication of the concentration of fine grains (ferrimagnetic magnetite/maghemite) that form during weathering and pedogenesis and heat[66]. Anhysteretic remanent magnetisation (ARM) was imparted using a DTECH alternating field demagnetizer with a peak alternating field of 100 mT and a direct current biasing field of 0.1 mT. Plotted values have been normalized for the direct current biasing field and expressed as $\chi_{ARM}$. Saturation isothermal remanent magnetization using a 1 T field, was generated by an MMPM5 Pulse Magnetiser. Reverse field demagnetization at fields of −20 mT, −40 mT, −100 mT and −300 mT was then performed and samples exposed directly to IRM reverse immediately after SIRM. All remanence measurements were made using a Molspin fluxgate spinner magnetometer with a noise level of $0.1 \times 10^{-8}$ A m. Results are described following previous studies[54,56,59,60].

The magnetic properties of sediment samples were analysed from the purported combustion feature in Area I East, three from the RCS and two from the adjacent unaltered substrate, the YBCS. A further sample of YBCS was taken for an experimental reference dataset to evaluate the impact of different heating processes on the magnetic properties.

The experimental design followed previous archaeomagnetic fire studies[49,67] to investigate: (1) whether the magnetic properties of the RCS arose from heating or natural processes (pedogenesis) and, if the former, (2) whether they resulted from multiple relighting events (anthropogenic) or from a single more extensive heating event (natural or anthropogenic). Owing to the large number of experiments required for this study and limited availability of archaeological substrate, we were only able to conduct laboratory-based experiments. Four main experiments were conducted and repeated using the YBCS, with stepwise incremental heating (from 100 °C to a maximum of 1,000 °C) for a range of heating durations (4 h up to 48 h) to compare with the archaeological results, and deduce whether they were heated and, if so, the duration and number of heating events (Supplementary Information, section 5).

### Polycyclic aromatic hydrocarbons

PAHs serve as biomolecular records for fire providing quantitative data on the natural occurrences and patterns of fire in various environments across geological timescales[68,69]. The PAHs produced during burning have different structures, for example, two to six rings. Previous research has shown that the production of PAHs varies when wood is burned, with those having a lower molecular weight (fewer than four rings) found predominantly in the gaseous phase, and those with a higher molecular weight (more than four rings) found in the particulate phase[70,71]. Archaeological evidence indicates that anthropogenic combustion features can reach temperatures sufficient to generate hPAHs, which have a higher molecular weight[72,73] and are less prone to travelling far from the fire's origin. Natural fires consistently have a greater presence of PAHs with lPAHs[28,72,74], which can travel long distances. Therefore, a high ratio of hPAHs/lPAHs is a good indication of human fire use[27].

Following established procedures[75], nine samples were collected from Area I East in 2022 using sterilized equipment, placed in precleaned polyethylene bags and frozen to −20 °C until analysis. Ultrasonically dispersed sediment samples (10 g) were mixed with recovery standards. The samples were then Soxhlet extracted for 24 h using a 200 ml mixture of hexane and dichloromethane (1:3, v:v). The sediment extract was concentrated to 4 ml using a rotary evaporator and purified with a silica gel and alumina column (2:1, v:v; 30 cm height × 10 mm internal diameter) with He as the carrier (1.5 ml $min^{-1}$). Each column containing the target PAHs was eluted with 70 ml of hexane and dichloromethane mixture (7:3, v:v), concentrated to 0.5 ml and spiked with internal standards before instrumental analysis. The total concentrations of the PAHs in the solutions were determined by

gas chromatography mass spectrometry using an Agilent 7890A gas chromatograph equipped with 5977B mass-selective detector and a 30 m DB-5MS fused silica capillary column (0.25 mm internal diameter, 0.25 mm film thickness). The oven temperature was ramped from 60 °C to 200 °C at 10 °C $min^{-1}$, then to 214 °C at 2 °C $min^{-1}$, followed by 254 °C at 5 °C $min^{-1}$ and finally to 290 °C at 18 °C $min^{-1}$. The temperature was held for 2 min at 254 °C and 17 min at 290 °C. Calibration standards and spiked and procedural blanks were included with every ten samples to ensure quality assurance and control. Normalization of PAH concentrations used the dry weight of extracted sediment[27,76,77] (Supplementary Information, section 6).

### Fourier-transform infrared spectroscopy

FTIR spectroscopy characterizes the molecular absorptions of infrared radiation by organic and inorganic material. As applied to archaeology, the resulting absorbance spectra can be used to understand the composition of sediments and materials. For Barnham, comparative experiments were performed to determine how composition and crystallography vary with heat alteration at different temperatures, and so provide a reference collection of FTIR responses[49,78].

Subsamples of the YBCS (sample 1084) from Area I, away from the purported fire feature in Area I East, but with the same mineralogical properties, were used in these experiments. Each subsample was heated in a porcelain crucible in a muffle furnace for 4 h, at temperatures ranging from 250 °C to 1,000 °C in 50 °C increments. A further two samples were heated to 150 and 200 °C in a laboratory oven. An unheated (oven-dried to 105 °C) sample was prepared for reference. Samples for both the heating experiment and FTIR analysis of the archaeological samples were prepared by grinding roughly 2–3 mg of sample in an agate mortar and pestle and mixing with 200 mg of potassium bromide. Around 80 mg of the mixture was then formed into a transparent disc using a hand press. A Thermo Nicolet iS10 spectrometer was used to analyse the samples and obtain spectra between 4,000 $cm^{-1}$ and 400 $cm^{-1}$, at 4 $cm^{-1}$ intervals. The FTIR reference collection of standard materials created by the Kimmel Centre of Archaeological Science, Weizmann Institute of Science (http://www.weizmann.ac.il/kimmel-arch/infrared-spectra-library.mel-arch/infrared-spectra-library) was used for comparison with the Barnham sample spectra.

Based on previous studies[79–81] and preliminary laboratory work it was expected that alterations due to heating would be detected in changes to kaolinite clay bands around 1,035 $cm^{-1}$, 915 $cm^{-1}$ and 533 $cm^{-1}$. The heating experiment was designed to determine the temperature of those alterations to construct a spectra library specific to the sediments at Barnham. Previous experimental work has shown that sediments containing different clay types produce different temperature responses, and thus the use of local sediments to construct site-specific spectra libraries was essential[80] (Supplementary Information, section 7).

### Pyrite XRD analysis and imaging

Micro-XRD was performed on the two pyrite nodule fragments using a Rigaku Dmax Rapid II Micro-XRD system. Several point analyses were collected on the outer cortical surfaces and internal fracture faces of each nodule, using a spot size diameter of approximately 900 µm. The XRD setup was configured with a copper X-ray source at 40 kV and 36 mA, a 300 µm collimator and a fixed incident X-ray beam of 20°. Data were collected using a curved two-dimensional imaging plate detector, and phase identification was based on comparison with standard references from the ICDD PDF-5+ diffraction database (https://www.icdd.com/pdf-5/).

High-resolution three-dimensional imaging of surface features was conducted using a focus variation microscope (Alicona InfiniteFocus G5+) with a ×4 lens. Imaging parameters included a working distance of 17.5 mm and a vertical resolution of 100 nm. Complementary surface detail was captured using a JEOL IT500 scanning electron microscope operated in variable pressure mode (approximately 70 Pa chamber pressure) (Supplementary Information, section 2).

### Clast lithological analysis

Identification of the lithology of clasts is used widely as a technique for understanding the geological source of stones in fluvial, marine or other gravel-rich deposits, which can help in understanding the processes involved in sediment formation as well as provide a means of correlation and differentiation of deposits, and reconstruction of landscape changes resulting from fluvial and glacial processes[82]. Geological work in the Breckland since 1987 has generated a large number of such studies, which provides a database of over 121,000 stone identifications from 29 sites or contexts (Supplementary Information, section 3). This enables an independent assessment of the prevalence of iron pyrite in the Breckland area, encompassing the three main Pleistocene sets of deposits: pre-MIS 12 Bytham River sediments; MIS 12 glacial sediments; post-MIS 12 fluvial sediments. Gravel samples are normally sieved to capture the 11.2–16.0 mm size fraction and, where clasts counts are low, the 8.0–11.2 mm size fraction are counted[83].

### Reporting summary

Further information on research design is available in the Nature Portfolio Reporting Summary linked to this article.

## Data availability

All data is presented in the Supplementary Information or is linked to Excel spreadsheets.


46. Mentzer, S. M. Microarchaeological approaches to the identification and interpretation of combustion features in prehistoric archaeological sites. *J. Archaeol. Meth. Theory* **21**, 616–668 (2014).
47. Barbetti, M. Traces of fire in the archaeological record, before one million years ago? *J. Hum. Evol.* **15**, 771–781 (1986).
48. Thieme, H. in *The Hominid Individual in Context: Archaeological Investigations of Lower and Middle Palaeolithic Landscapes, Locales and Artefacts* (eds Gamble, C. & Porr, M.) 115–132 (Routledge, 2005).
49. Stahlschmidt, M. C. et al. On the evidence for human use and control of fire at Schöningen. *J. Hum. Evol.* **89**, 181–201 (2015).
50. Stoops, G. *Guidelines for Analysis and Description of Soil and Regolith Thin Sections* (Soil Science Society of America, 2003).
51. Stoops, G. *Guidelines for Analysis and Description of Soil and Regolith Thin Sections* (Wiley, 2021).
52. Herries, A. I. & Fisher, E. C. Multidimensional GIS modelling of magnetic mineralogy as a proxy for fire use and spatial patterning: evidence from the Middle Stone Age bearing sea cave of Pinnacle Point 13B (Western Cape, South Africa). *J. Hum. Evol.* **59**, 306–320 (2010).
53. Herrejón Lagunilla, Á et al. An experimental approach to the preservation potential of magnetic signatures in anthropogenic fires. *PLoS ONE* **14**, e0221592 (2019).
54. Oldfield, F. & Crowther, J. Establishing fire incidence in temperate soils using magnetic measurements. *Palaeogeog. Palaeoclim. Palaeoecol.* **249**, 362–369 (2007).
55. Gedye, S. J. et al. The use of mineral magnetism in the reconstruction of fire history: a case study from Lago di Origlio, Swiss Alps. *Palaeogeog. Palaeoclim. Palaeoecol.* **164**, 101–110 (2000).
56. Dearing, J. A. in *Environmental Magnetism: a Practical Guide* (eds Walden, J. et al.) 25–62 (Quaternary Research Association, 1999).
57. Maher, B. A. The magnetic properties of some synthetic submicron magnetites. *Geophys. J. R. Astron. Soc.* **94**, 83–96 (1988).
58. Maki, D., Homburg, J. A. & Brosowske, S. D. Thermally activated mineralogical transformations in archaeological hearths: inversion from maghemite γFe2O4 phase to haematite αFe2O4 form. *Archaeolog. Prospec.* **13**, 207–227 (2006).
59. Liu, Q. et al. Environmental magnetism: principles and applications. *Rev. Geophys.* **50**, 2–50 (2012).
60. Thompson, R. & Oldfield, F. *Environmental Magnetism* (Allen and Unwin, 1986).
61. Linford, N. T. & Canti, M. G. Geophysical evidence for fires in antiquity: preliminary results from an experimental study. Paper given at the EGS XXIV General Assembly in The Hague, April 1999. *Archaeol. Prospec.* **8**, 211–225 (2001).
62. Ketterings, Q. M., Bigham, J. M. & Laperche, V. Changes in soil mineralogy and texture caused by slash-and-burn fires in Sumatra, Indonesia. *Soil Sci. Soc. Am. J.* **64**, 1108–1117 (2000).
63. Pulley, S., Lagesse, J. & Ellery, W. The mineral magnetic signatures of fire in the Kromrivier wetland, South Africa. *J. Soils Sed.* **17**, 1170–1181 (2017).
64. Walden, J., Oldfield, F. & Smith, J. P. (eds) *Environmental Magnetism: a Practical Guide* (Quaternary Research Association, 1999).
65. Worm, H. U. On the superparamagnetic–stable single domain transition for magnetite, and frequency dependence of susceptibility. *Geophys. J. Int.* **133**, 201–206 (1988).

66. Blundell, A. et al. Controlling factors for the spatial variability of soil magnetic susceptibility across England and Wales. *Earth Sci. Rev.* **95**, 158–188 (2009).
67. Snape, L. & Church, M. J. in *Wild Things 2.0: Further Advances in Palaeolithic and Mesolithic Research* (eds Walker, J. & Clinnick, D.) 55–80 (Oxbow Books, 2019).
68. Karp, A. T. et al. Fire distinguishers: refined interpretations of polycyclic aromatic hydrocarbons for paleo-applications. *Geochim. Cosmochim. Acta* **289**, 93–113 (2020).
69. Song, Y. et al. Distribution of pyrolytic PAHs across the Triassic–Jurassic boundary in the Sichuan Basin, southwestern China: evidence of wildfire outside the Central Atlantic Magmatic Province. *Earth Sci. Rev.* **201**, 102970 (2020).
70. Hytönen, K. et al. Gas–particle distribution of PAHs in wood combustion emission determined with annular denuders, filter, and polyurethane foam adsorbent. *Aerosol Sci. Tech.* **43**, 442–454 (2009).
71. McDonald, J. D. et al. Fine particle and gaseous emission rates from residential wood combustion. *Environ. Sci. Tech.* **34**, 2080–2091 (2000).
72. Hoare, S. Assessing the function of Palaeolithic hearths: experiments on intensity of luminosity and radiative heat outputs from different fuel sources. *J. Paleol. Archaeol.* **3**, 537–565 (2020).
73. Argiriadis, E. et al. Lake sediment fecal and biomass burning biomarkers provide direct evidence for prehistoric human-lit fires in New Zealand. *Sci. Rep.* **8**, 12113 (2018).
74. Campos, I. & Abrantes, N. Forest fires as drivers of contamination of polycyclic aromatic hydrocarbons to the terrestrial and aquatic ecosystems. Curr. *Opin. Environ. Sci. Health* **24**, 100293 (2021).
75. Sojinu, O. S., Sonibare, O. O. & Zeng, E. Y. Concentrations of polycyclic aromatic hydrocarbons in soils of a mangrove forest affected by forest fire. *Toxicolog. Environ. Chem.* **93**, 450–461 (2011).
76. Yunker, M. B. et al. PAHs in the Fraser River basin: a critical appraisal of PAH ratios as indicators of PAH source and composition. *Org. Geochem.* **33**, 489–515 (2002).
77. Faboya, O. L. et al. Impact of forest fires on polycyclic aromatic hydrocarbon concentrations and stable carbon isotope compositions in burnt soils from tropical forest, Nigeria. *Sci. Afr.* **8**, e00331 (2020).
78. Weiner, S. *Microarchaeology-Beyond the Visible Archaeological Record* (Cambridge Univ. Press, 2010).
79. Madejova, J. & Komadel, P. Baseline studies of the Clay Mineral Society source clays: infrared methods. *Clays Clay Min.* **49**, 410–432 (2001).
80. Berna, F. et al. Sediments exposed to high temperatures: reconstructing pyrotechnological processes in Late Bronze and Iron Age strata at Tel dor (Israel). *J. Archaeol. Sci.* **34**, 358–373 (2007).
81. Saikia, B. J. & Parthasarathy, G. Fourier transform infrared spectroscopic characterization of kaolinite from Assam and Meghalaya, Northeastern India. *J. Mod. Phys.* **1**, 206–210 (2010).
82. Bridgland, D. R. *Clast Lithological Analysis. Technical Guide No. 3* (Quaternary Research Association, 1986).
83. Gale, S. J. & Hoare, P. G. *Quaternary Sediments: Petrographic Methods for the Study of Unlithified Rocks* (Blackburn, 2011).

**Acknowledgements** We would like to thank M. Stahlschmidt for the analysis and interpretation of initial work on the micromorphology and invaluable assistance to S.H. on the additional thin sections. We are grateful to C. Jeans and W. Lord for discussions on the pyrite. We also thank C. Williams for help with the illustrations. Access to the site on the Euston Estate has been provided by the Duke of Grafton and the Heading family, and we are grateful to M. Hawthorne, D. Heading, E. Heading and R. Heading for their ready assistance throughout the fieldwork. Further logistical support has been provided by D. Switzer of PR International. We thank the excavation and post-excavation teams, in particular L. Dale, X. Ding, S. Hunter, D. Jones, I. Klipsch, M. Özturan, A. Rawlinson and I. Taylor, and site manager T. B. Jones. The research was supported by the Calleva Foundation through the Pathways to Ancient Britain project and for S.M.B. through the Human Prehistoric Behaviour in 3D project, and the paper is a contribution to the Natural History Museum's Evolution of Life research theme.

**Author contributions** R.D., N.A., S.M.B., M.H., S.H., S.G.L., J.M., J.N., S.O.'C., S.A.P., A.S. and C.S. wrote the paper. R.D., N.A. and C.L. analysed the artefacts. M.L. and S.P. were responsible for palynology. S.H. performed micromorphology and environmental magnetism experiments, and analysed PAHs. M.H. performed FTIR spectroscopy. S.M.B., J.N., S.A.P. and A.S. analysed pyrites. S.G.L. and N.A. performed lithological analyses. J.M. performed photogrammetry and photography.

**Competing interests** The authors declare no competing interests.

**Additional information**
**Supplementary information** The online version contains supplementary material available at https://doi.org/10.1038/s41586-025-09855-6.
**Correspondence and requests for materials** should be addressed to Nick Ashton.
**Peer review information** *Nature* thanks Susan Mentzer, Ségolène Vandevelde and the other, anonymous, reviewer(s) for their contribution to the peer review of this work. Peer reviewer reports are available.

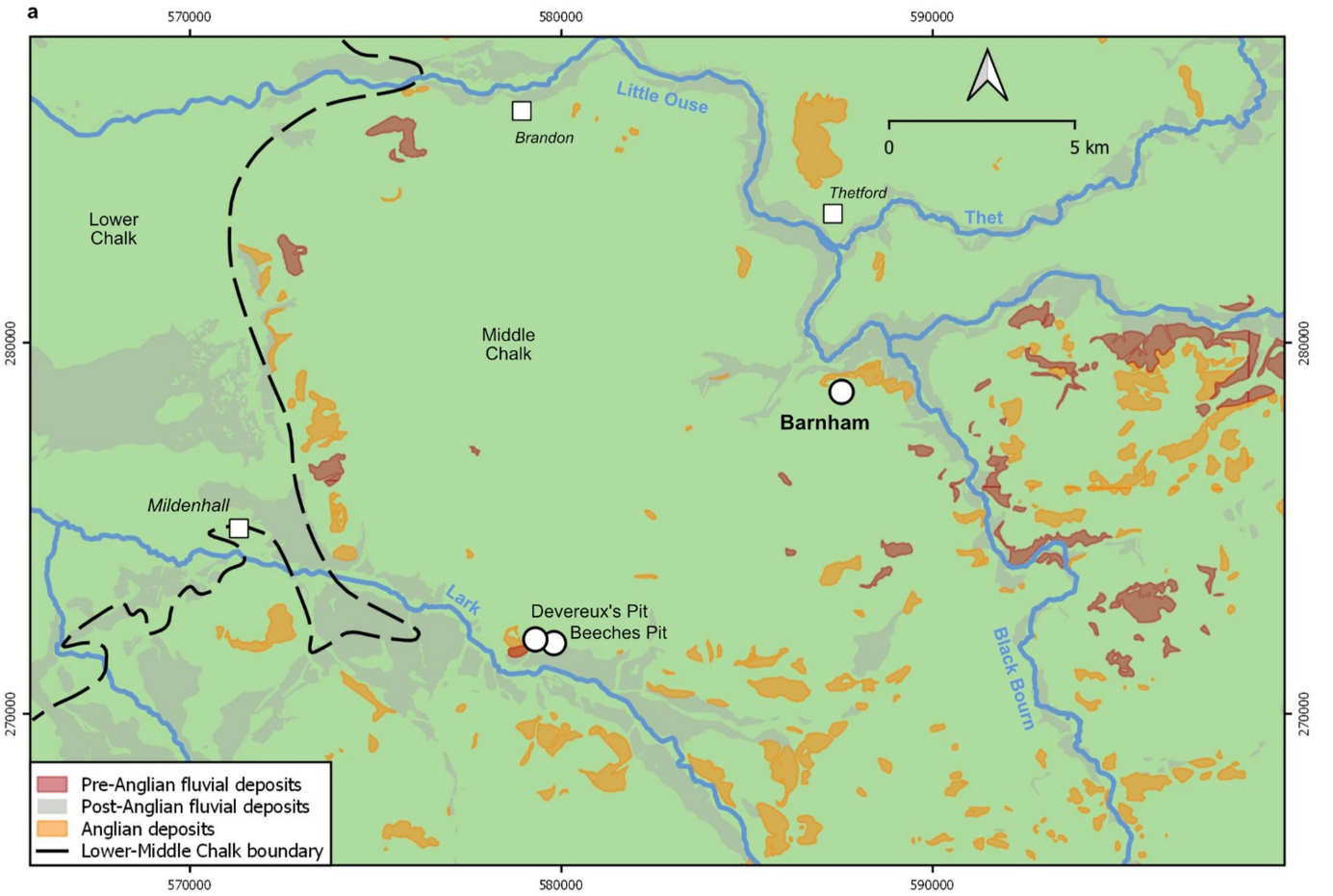


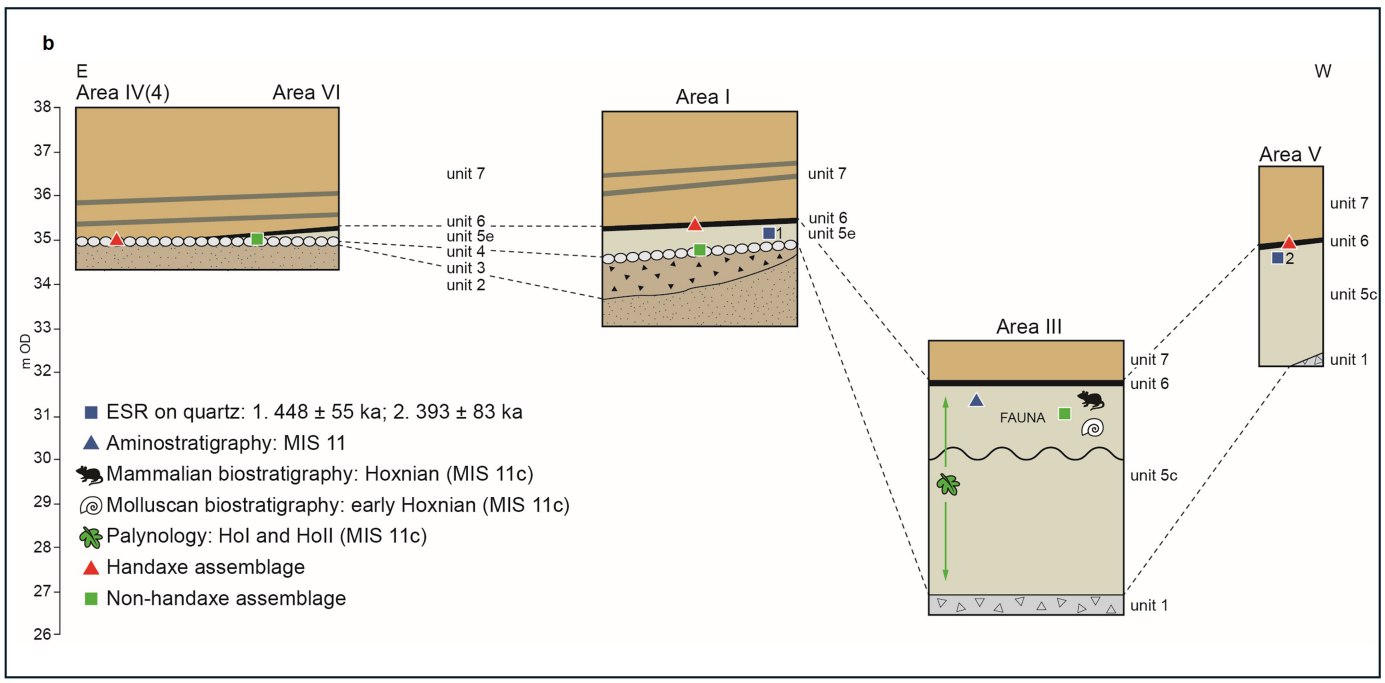


**Extended Data Fig. 1** | See next page for caption.

**Extended Data Fig. 1 | Geology of Barnham. a**. Map of the Breckland area showing sites of Barnham, Beeches Pit and Devereux's Pit. Also shown is the boundary of the Lower and Middle Chalk and key superficial deposits discussed in the text. **b**. Schematic cross-section of the sedimentary sequence at East Farm Barnham, showing locations of samples for dating, biostratigraphy, palynology and contexts containing archaeology. Units 1–3 = glacial sediments; unit 4 = lag gravel; unit 5 = lacustrine sediments with lateral transition between unit 5c in the middle of the basin and unit 5e on the edge; unit 6 = palaeosol; unit 7 = brickearth. Credits: Panel **a** contains public sector information licensed under the Open Government Licence v.3.0 (British Geological Survey UKRI, 2025). Panel **b** created by C. Williams.

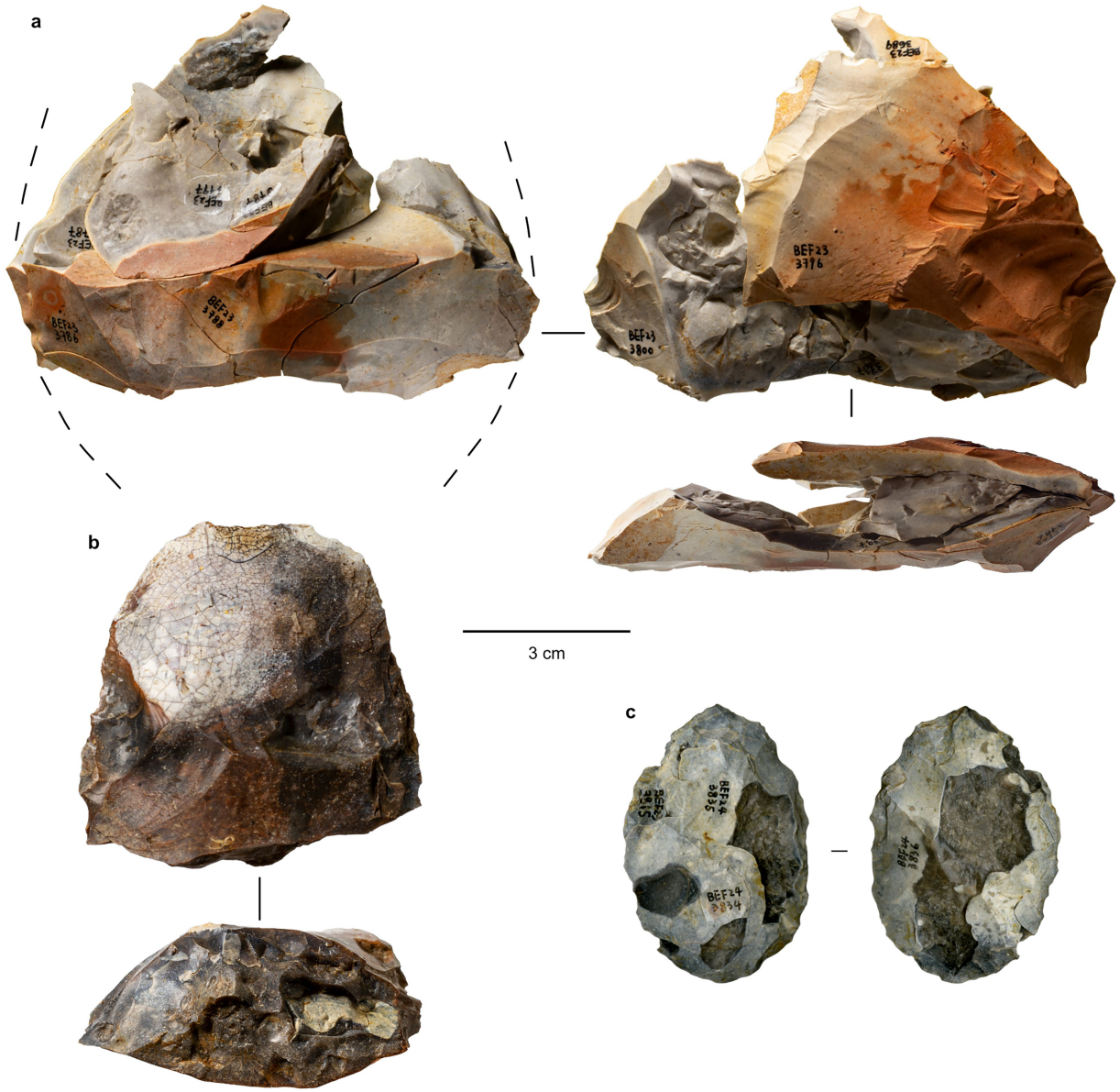


**Extended Data Fig. 2 | Heat shattered handaxes from Barnham. a**. Central part of heat-shattered handaxe with 25 refitting pieces excavated from within a small zone (35 cm across) in Area I East. **b**. Top part of heat-shattered handaxe from Area I East. **c**. Heat-altered handaxe from Area I East.

nature portfolio

Corresponding author(s): Nick Ashton

Last updated by author(s): 13th October 2025

# Reporting Summary

Nature Portfolio wishes to improve the reproducibility of the work that we publish. This form provides structure for consistency and transparency in reporting. For further information on Nature Portfolio policies, see our Editorial Policies and the Editorial Policy Checklist.

Please do not complete any field with "not applicable" or n/a. Refer to the help text for what text to use if an item is not relevant to your study.
For final submission: please carefully check your responses for accuracy; you will not be able to make changes later.

## Statistics

For all statistical analyses, confirm that the following items are present in the figure legend, table legend, main text, or Methods section.

| n/a | Confirmed | |
|---|---|---|
| ☐ | ☒ | The exact sample size (*n*) for each experimental group/condition, given as a discrete number and unit of measurement |
| ☒ | ☐ | A statement on whether measurements were taken from distinct samples or whether the same sample was measured repeatedly |
| ☐ | ☒ | The statistical test(s) used AND whether they are one- or two-sided<br>*Only common tests should be described solely by name; describe more complex techniques in the Methods section.* |
| ☐ | ☒ | A description of all covariates tested |
| ☒ | ☐ | A description of any assumptions or corrections, such as tests of normality and adjustment for multiple comparisons |
| ☐ | ☒ | A full description of the statistical parameters including central tendency (e.g. means) or other basic estimates (e.g. regression coefficient) AND variation (e.g. standard deviation) or associated estimates of uncertainty (e.g. confidence intervals) |
| ☐ | ☒ | For null hypothesis testing, the test statistic (e.g. *F*, *t*, *r*) with confidence intervals, effect sizes, degrees of freedom and *P* value noted<br>*Give P values as exact values whenever suitable.* |
| ☒ | ☐ | For Bayesian analysis, information on the choice of priors and Markov chain Monte Carlo settings |
| ☒ | ☐ | For hierarchical and complex designs, identification of the appropriate level for tests and full reporting of outcomes |
| ☒ | ☐ | Estimates of effect sizes (e.g. Cohen's *d*, Pearson's *r*), indicating how they were calculated |

*Our web collection on statistics for biologists contains articles on many of the points above.*

## Software and code

Policy information about availability of computer code

Data collection

Data analysis

For manuscripts utilizing custom algorithms or software that are central to the research but not yet described in published literature, software must be made available to editors and reviewers. We strongly encourage code deposition in a community repository (e.g. GitHub). See the Nature Portfolio guidelines for submitting code & software for further information.

## Data

Policy information about availability of data

All manuscripts must include a data availability statement. This statement should provide the following information, where applicable:

- Accession codes, unique identifiers, or web links for publicly available datasets
- A description of any restrictions on data availability
- For clinical datasets or third party data, please ensure that the statement adheres to our policy

A data availability statement is included

## Research involving human participants, their data, or biological material

Policy information about studies with human participants or human data. See also policy information about sex, gender (identity/presentation), and sexual orientation and race, ethnicity and racism.

| | |
|---|---|
| Reporting on sex and gender | |
| Reporting on race, ethnicity, or other socially relevant groupings | |
| Population characteristics | |
| Recruitment | |
| Ethics oversight | |

Note that full information on the approval of the study protocol must also be provided in the manuscript.

# Field-specific reporting

Please select the one below that is the best fit for your research. If you are not sure, read the appropriate sections before making your selection.

☐ Life sciences ☐ Behavioural & social sciences ☒ Ecological, evolutionary & environmental sciences

For a reference copy of the document with all sections, see nature.com/documents/nr-reporting-summary-flat.pdf

# Life sciences study design

All studies must disclose on these points even when the disclosure is negative.

| | |
|---|---|
| Sample size | |
| Data exclusions | |
| Replication | |
| Randomization | |
| Blinding | |

# Behavioural & social sciences study design

All studies must disclose on these points even when the disclosure is negative.

| | |
|---|---|
| Study description | |
| Research sample | |
| Sampling strategy | |
| Data collection | |
| Timing | |
| Data exclusions | |
| Non-participation | |
| Randomization | |

## Ecological, evolutionary & environmental sciences study design

All studies must disclose on these points even when the disclosure is negative.

| | |
|---|---|
| Study description | Excavation at East Farm Pit, Barnham, UK |
| Research sample | Artefacts, sediment samples for micromorphology, Magnetics, PAH and FTIR |
| Sampling strategy | Column sample through reddened clayey silt, comparative sample from unreddened sediment |
| Data collection | Excavation by hand |
| Timing and spatial scale | 2022-2024 |
| Data exclusions | |
| Reproducibility | Sediments can be resampled |
| Randomization | |
| Blinding | |

Did the study involve field work? [X] Yes [ ] No

## Field work, collection and transport

| | |
|---|---|
| Field conditions | Overgrown, disused claypit, UK. Summer |
| Location | East Farm Pit, Barnham, Suffolk, UK |
| Access & import/export | n/a |
| Disturbance | n/a |

# Reporting for specific materials, systems and methods

We require information from authors about some types of materials, experimental systems and methods used in many studies. Here, indicate whether each material, system or method listed is relevant to your study. If you are not sure if a list item applies to your research, read the appropriate section before selecting a response.

### Materials & experimental systems

| n/a | Involved in the study |
|---|---|
| [X] | [ ] Antibodies |
| [X] | [ ] Eukaryotic cell lines |
| [ ] | [X] Palaeontology and archaeology |
| [X] | [ ] Animals and other organisms |
| [X] | [ ] Clinical data |
| [X] | [ ] Dual use research of concern |
| [X] | [ ] Plants |

### Methods

| n/a | Involved in the study |
|---|---|
| [X] | [ ] ChIP-seq |
| [X] | [ ] Flow cytometry |
| [X] | [ ] MRI-based neuroimaging |

## Antibodies

| | |
|---|---|
| Antibodies used | |
| Validation | |

## Eukaryotic cell lines

Policy information about cell lines and Sex and Gender in Research

| | |
|---|---|
| Cell line source(s) | |
| Authentication | |
| Mycoplasma contamination | |
| Commonly misidentified lines (See ICLAC register) | |

## Palaeontology and Archaeology

| | |
|---|---|
| Specimen provenance | Flint artefacts, pyrite - East Farm Pit, Barnham, Suffolk, UK |
| Specimen deposition | British Museum |
| Dating methods | |

[X] Tick this box to confirm that the raw and calibrated dates are available in the paper or in Supplementary Information.

| | |
|---|---|
| Ethics oversight | |

Note that full information on the approval of the study protocol must also be provided in the manuscript.

## Animals and other research organisms

Policy information about studies involving animals; ARRIVE guidelines recommended for reporting animal research, and Sex and Gender in Research

| | |
|---|---|
| Laboratory animals | |
| Wild animals | |
| Reporting on sex | |
| Field-collected samples | |
| Ethics oversight | |

Note that full information on the approval of the study protocol must also be provided in the manuscript.

## Clinical data

Policy information about clinical studies

All manuscripts should comply with the ICMJE guidelines for publication of clinical research and a completed CONSORT checklist must be included with all submissions.

| | |
|---|---|
| Clinical trial registration | |
| Study protocol | |
| Data collection | |
| Outcomes | |

## Dual use research of concern

Policy information about dual use research of concern

### Hazards

Could the accidental, deliberate or reckless misuse of agents or technologies generated in the work, or the application of information presented in the manuscript, pose a threat to:

| No | Yes | |
|---|---|---|
| X | ☐ | Public health |
| X | ☐ | National security |
| X | ☐ | Crops and/or livestock |
| X | ☐ | Ecosystems |
| X | ☐ | Any other significant area |

### Experiments of concern

Does the work involve any of these experiments of concern:

| No | Yes | |
|---|---|---|
| X | ☐ | Demonstrate how to render a vaccine ineffective |
| X | ☐ | Confer resistance to therapeutically useful antibiotics or antiviral agents |
| X | ☐ | Enhance the virulence of a pathogen or render a nonpathogen virulent |
| X | ☐ | Increase transmissibility of a pathogen |
| X | ☐ | Alter the host range of a pathogen |
| X | ☐ | Enable evasion of diagnostic/detection modalities |
| X | ☐ | Enable the weaponization of a biological agent or toxin |
| X | ☐ | Any other potentially harmful combination of experiments and agents |

## Plants

Seed stocks

Novel plant genotypes

Authentication

## ChIP-seq

### Data deposition

☐ Confirm that both raw and final processed data have been deposited in a public database such as GEO.

☐ Confirm that you have deposited or provided access to graph files (e.g. BED files) for the called peaks.

Data access links
*May remain private before publication.*

Files in database submission

Genome browser session
(e.g. UCSC)

### Methodology

Replicates

Sequencing depth

Antibodies

Peak calling parameters

Data quality

Software

## Flow Cytometry

### Plots

Confirm that:

☐ The axis labels state the marker and fluorochrome used (e.g. CD4-FITC).

☐ The axis scales are clearly visible. Include numbers along axes only for bottom left plot of group (a 'group' is an analysis of identical markers).

☐ All plots are contour plots with outliers or pseudocolor plots.

☐ A numerical value for number of cells or percentage (with statistics) is provided.

### Methodology

Sample preparation

Instrument

Software

Cell population abundance

Gating strategy

☐ Tick this box to confirm that a figure exemplifying the gating strategy is provided in the Supplementary Information.

## Magnetic resonance imaging

### Experimental design

Design type

Design specifications

Behavioral performance measures

Imaging type(s)

Field strength

Sequence & imaging parameters

Area of acquisition

Diffusion MRI ☐ Used ☐ Not used

### Preprocessing

Preprocessing software

Normalization

Normalization template

Noise and artifact removal

Volume censoring

### Statistical modeling & inference

Model type and settings

Effect(s) tested

Specify type of analysis: ☐ Whole brain ☐ ROI-based ☐ Both

Statistic type for inference

(See Eklund et al. 2016)

Correction

## Models & analysis

| n/a | Involved in the study |
|---|---|
| ☐ | ☐ Functional and/or effective connectivity |
| ☐ | ☐ Graph analysis |
| ☐ | ☐ Multivariate modeling or predictive analysis |

Functional and/or effective connectivity

Graph analysis

Multivariate modeling and predictive analysis